ChemPlusChem

Research Article
doi.org/10.1002/cplu.202400340

Chemistry Europe
European Chemical Societies Publishing

www.chempluschem.org

Structure and Conformation Determine Gas-Phase Infrared Spectra of Detergents

Carla Kirschbaum,*[a] Kim Greis,[b] Sandy Gewinner,[c] Wieland Schöllkopf,[c] Gerard Meijer,[c] Gert von Helden,[c] Kevin Pagel,[c, d] and Leonhard H. Urner*[e]

Native mass spectrometry of membrane proteins relies on non-ionic detergents which protect the protein during transfer from solution into the gas phase. Once in the gas phase, the detergent micelle must be efficiently removed, which is usually achieved by collision-induced dissociation (CID). Recently, infrared multiple photon dissociation (IRMPD) has emerged as an alternative activation method for the analysis of membrane proteins, which has led to a growing interest in detergents that efficiently absorb infrared light. Here we investigate whether the absorption properties of synthetic detergents can be tailored by merging structural motifs of existing detergents into new hybrid detergents. We combine gas-phase infrared ion spectroscopy with density functional theory to investigate and rationalize the absorption properties of three established detergents and two hybrid detergents with fused headgroups. We show that, although the basic intramolecular interactions in the parent and hybrid detergents are similar, the three-dimensional structures differ significantly and so do the infrared spectra. Our results outline a roadmap for guiding the synthesis of tailored detergents with computational chemistry for future mass spectrometry applications.

Introduction

Non-ionic detergents enable the native mass spectrometry (nMS) analysis of intact membrane protein complexes.[1] Detergents are required for both the solubilization of hydrophobic membrane proteins and the protection of non-covalent protein interactions during transfer from solution into the vacuum of a mass spectrometer.[2] nMS is a powerful analytical technique which can inform on protein complex identity, composition, dissociation pathways, ligand binding, and the role of ligands in protein oligomerization.[3]

The advent of nMS of membrane proteins was supported by the development of detergents with customizable solution and gas-phase properties.[3] A key challenge in nMS is to chemically design detergents that stabilize proteins in solution and can be removed under gentle conditions inside a mass spectrometer to maintain non-covalent protein interactions prior to mass analysis.[3b] Saccharide detergents, such as *n*-dodecyl-β-D-maltoside or *n*-octyl-β-D-glucoside (OG), stabilize proteins well in solution but require a high energy input for detergent removal in vacuum.[4] Tetraethylene glycol monooctyl ether (C8E4) does not stabilize proteins well in solution but is readily removed in vacuum.[4] More recently, first-generation, dendritic triglycerol detergent [G1] OGD and asymmetric hybrid detergents **1** and **2** were designed to integrate favourable solution and gas-phase properties (Figure 1).[5]

A complementary solution to the detergent removal problem is the development of MS activation methods, which include collision-induced dissociation (CID) and infrared multiple photon dissociation (IRMPD). Today, detergents are commonly removed from protein complexes by CID.[2,6] Forced by an electric field, protein-detergent complexes collide with neutral gas molecules. The internal energy of the complexes rises and dissipates through the dissociation of non-covalent bonds, which includes detergent removal, subunit dissociation, and/or protein unfolding.[7] Detergents that preferably guide energy dissipation through the detergent removal pathway can help to maintain non-covalent protein interactions.[7] Detergent design parameters that serve this purpose include non-ionic character, five hydroxyl groups or less in the detergent head, a hydrophilic-lipophilic balance between 11 and 17, and a critical micelle concentration in the lower micromolar range.[3b,8]

Less is known about the design of detergents that can be removed with IRMPD.[9] Here, protein-detergent complexes are irradiated with infrared (IR) light (typically 10.6 μm wavelength for CO_2 lasers), and the sequential absorption of multiple photons followed by intramolecular vibrational redistribution

[a] C. Kirschbaum
Kavli Institute for Nanoscience Discovery, University of Oxford, South Parks Rd., Oxford OX1 3QU, United Kingdom
E-mail: carla.kirschbaum@chem.ox.ac.uk

[b] K. Greis
Department of Chemistry and Applied Biosciences, ETH Zürich, Vladimir-Prelog-Weg 10, 8093 Zürich, Switzerland

[c] S. Gewinner, W. Schöllkopf, G. Meijer, G. von Helden, K. Pagel
Fritz Haber Institute of the Max Planck Society, Faradayweg 4-6, 14195 Berlin, Germany

[d] K. Pagel
Department of Chemistry and Biochemistry, Freie Universität Berlin, Altensteinstraße 23a, 14195 Berlin, Germany

[e] L. H. Urner
Department of Chemistry and Chemical Biology, TU Dortmund University, Otto-Hahn-Str. 6, 44227 Dortmund, Germany
E-mail: leonhard.urner@tu-dortmund.de

Supporting information for this article is available on the WWW under https://doi.org/10.1002/cplu.202400340

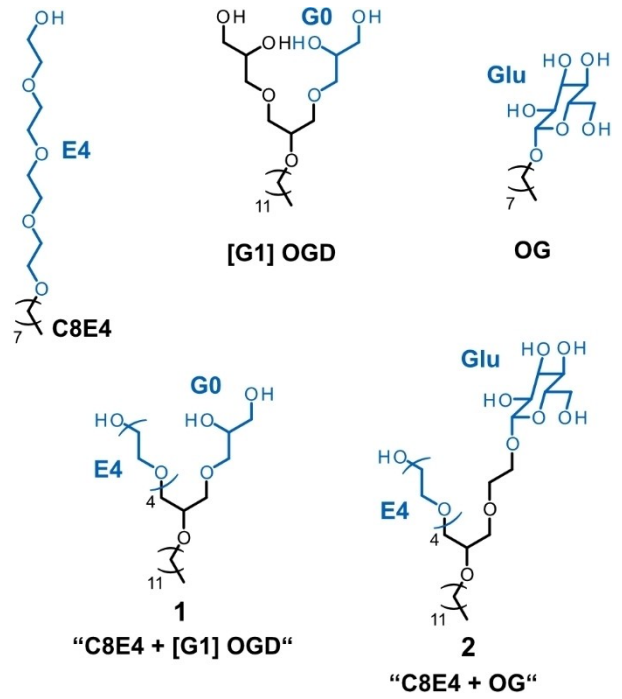

Figure 1. Overview of detergent structures. Molecular structures of asymmetric hybrid detergents **1** and **2** contain headgroup elements of C8E4, [G1] OGD, and OG.

(IVR) leads to a gradual increase in the internal ion energy, eventually resulting in dissociation of protein-detergent interactions. Like CID, IRMPD is suitable to release intact membrane proteins from detergent micelles and can retain non-covalent protein-lipid interactions.[9a] Major advantages of IRMPD over CID include charge-state-independent absorption of photons and a high degree of control in tuning the irradiation time and radiation intensity.[9c] Detergents with IR absorption bands that match the wavelength of IRMPD lasers could increase the efficiency of detergent evaporation and hence facilitate protein release for MS analysis.[9c] Therefore, detergents with favourable absorption properties are currently being sought.

Knowledge on how to chemically design non-ionic detergents with IR absorptions that overlap with the wavelength of the IR laser remains elusive. Herein, we combine modular detergent chemistry, gas-phase IR ion spectroscopy, and computational chemistry to explore experimental capabilities in designing detergents with customizable gas-phase IR absorption properties. Specifically, we investigate whether the gas-phase IR absorption properties of the detergents C8E4, [G1] OGD, and OG can be combined by fusing their IR-active functional groups into hybrid detergents **1** and **2** (Figure 1).

Results and Discussion

Hybrid Detergent Design

Gas-phase IR absorption properties of detergents are mainly determined by the structure of their polar headgroups.[9c] To understand how gas-phase IR spectra of detergents change when their headgroups are covalently combined, we designed hybrid detergents **1** and **2** (Figure 1). Specifically, we fused a glycerol fragment (**G0**) of the first-generation, dendritic triglycerol detergent [G1] OGD and the tetraethylene glycol head (**E4**) of C8E4 into hybrid detergent **1**. Furthermore, we fused the glucose head (**Glu**) of *n*-octyl-β-D-glucoside (OG) and the tetraethylene glycol head (**E4**) of C8E4 into hybrid detergent **2**. The synthesis of hybrid detergents **1** and **2** was accomplished by means of a previously established combinatorial dichloride coupling strategy.[10] Alternative synthesis strategies, such as triazole coupling,[11] Ugi-reaction,[12] or thiol-ene click[8] would also enable the fusion of different headgroups into hybrid detergents. However, the molecular structures of the parent detergents C8E4, [G1] OGD, and OG do not contain functional groups that result from these coupling procedures, including amide, triazole, and thioether. These functional groups have higher gas-phase basicity values compared to functional groups present in the parent detergents, i.e., ether, hydroxyl group, methylene groups.[13] Increasing the gas-phase basicity of functional groups alters not only the population of available protonation sites but also IR spectra of ionized species.[14] To minimize the bias on obtainable IR spectra, from a modular chemistry perspective, we excluded all functional groups in our design of hybrid detergents **1** and **2** other than those present in C8E4, [G1] OGD, and OG.

Gas-Phase Infrared Ion Spectroscopy

Having designed hybrid detergents **1** and **2**, we explored whether their gas-phase IR absorption properties reflect a combination of the parent detergents C8E4, [G1] OGD, and OG using gas-phase IR ion spectroscopy. This technique combines mass spectrometry and IR spectroscopy to generate IR spectra of isolated ions in the gas phase. Here we use an instrument employing superfluid helium as a spectroscopic matrix, which has been described previously (Figure 2).[15]

The detergents are ionized using nano-electrospray ionization, which is a soft ionization technique that generates mainly protonated, ammoniated, and sodiated detergent ions in positive ion mode (Figure S1). Mass spectrometry is used to

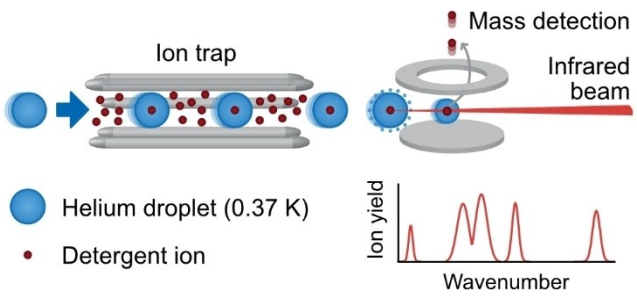

Figure 2. Schematic overview of gas-phase infrared spectroscopy in superfluid helium droplets. Detergent ions are picked up from an ion trap by helium droplets and are released from the droplets by irradiation with infrared light. The amount of released ions at each wavenumber is an indirect measure for light absorption.

determine the mass-to-charge ratio (*m/z*) of each ion type (Figure 3A). To measure the IR spectra of protonated detergents, only the *m/z* of interest is transferred into the instrument using a mass-selective quadrupole. The selected ions are then transferred into a temperature-controlled hexapole ion trap that is cooled to 90 K by liquid nitrogen. After thermalization, the ions are picked up from the trap by a beam of superfluid helium droplets that traversed the trap coaxially. Superfluid helium is used as a spectroscopic matrix because it is IR-transparent, cryogenic (0.4 K), and allows free vibrations of encapsulated ions.[16] The ion-doped droplets are irradiated with IR light provided by the Fritz Haber Institute free-electron laser,[17] which leads to vibrational excitation of the encapsulated ions if the light frequency is resonant with a vibrational transition. The absorbed energy is dissipated by evaporation of the helium shell, until the ions are eventually released from the droplets and detected by a mass spectrometer. This process requires more than 100 photons per droplet under the employed experimental conditions. The number of released ions at each wavelength is an indirect measure for IR absorption. Because the method is based on a non-linear photon absorption process, relative intensities in the IR spectra do not perfectly reproduce spectra obtained from linear IR spectroscopy methods, but are usually qualitatively comparable.[18]

Gas-phase IR spectroscopy in superfluid helium droplets achieves high resolution. Contrary to condensed-phase IR spectroscopy, the ions are free from intermolecular interactions. Furthermore, pre-cooling of ions in the ion trap leads to annealing of higher-energy conformers, which reduces the conformational flexibility and thus spectral complexity. Lastly, evaporative cooling by the helium matrix allows the ion to relax back into its vibrational ground state after each photon absorption, which considerably reduces thermal broadening of absorption bands.[19]

The fact that individual ions are probed in isolation holds an additional advantage over condensed-phase IR spectroscopy: the obtained IR spectra reflect intrinsic quantum-chemical properties of the ions, which can be computed *in silico*. By matching the experimental IR spectra with computed IR spectra of different conformers, information on the three-dimensional molecular structure and intramolecular interactions can be obtained.

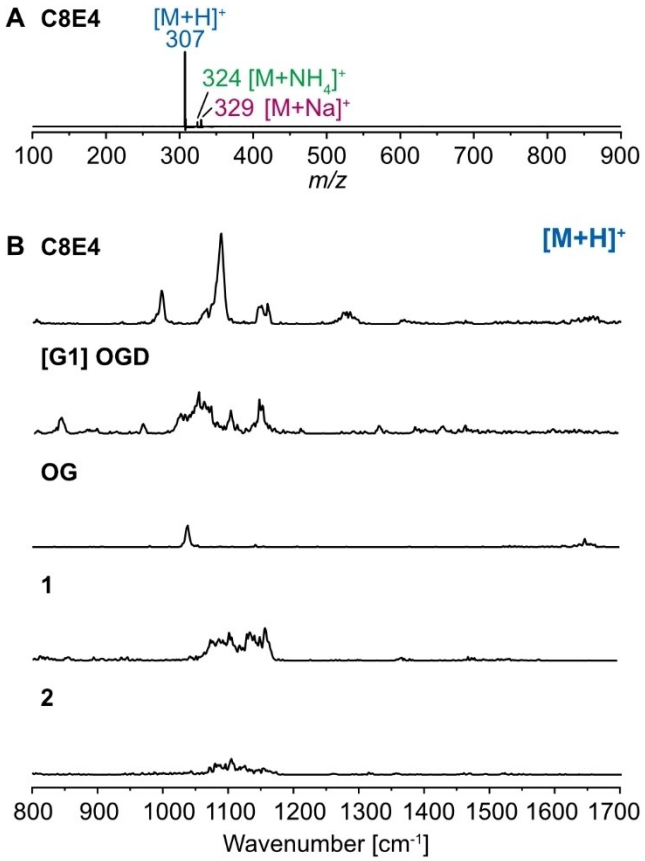

Figure 3. A) Mass spectrum of C8E4 with proton, ammonium, and sodium adducts highlighted. **B)** Gas-phase infrared spectra of protonated detergents. The intensities are scaled to the absorption maximum of the IR spectrum of protonated C8E4.

Infrared Spectra

For this study, we measured IR spectra of protonated detergents. The gas-phase IR spectra of all parent and hybrid detergents are displayed in the range from 800–1700 cm^{-1} in Figure 3B. All spectra have their most intense vibrations located between 1000–1200 cm^{-1}, which is the typical range of C–O and C–C stretching vibrations. Low-intensity peaks in the range between 1200–1500 cm^{-1} are typical for C–H bending vibrations of alkyl chains. In the spectrum of OG, and in most spectra with reduced intensity, an additional weak absorption band is visible between 1600–1700 cm^{-1}.

Because the most intense vibrations of all detergents lie in the range of commercial 9.3 μm (ca. 1075 cm^{-1}) CO_2 lasers, the latter might be a promising alternative to the more common 10.6 μm lasers (ca. 940 cm^{-1}) for detergent removal in native MS. It remains to be tested experimentally whether shorter-wavelength CO_2 lasers indeed increase the detergent removal efficiency or rather damage embedded proteins that also absorb in this range. We speculate that IVR within the protein-detergent complex prevents protein damage and enhances detergent release by inducing preferential dissociation of non-covalent protein-detergent bonds.

In addition to the absorption wavelength, the absolute absorption intensity is an important factor to consider for applications in nMS of membrane proteins. The absorption maximum in the IR spectrum of C8E4 serves as ideal benchmark for comparison since this detergent requires less IR irradiation intensity to be removed from membrane protein ions than any other detergent tested to date.[9c] The measured absorption intensities in the IR spectra obtained from hybrid detergents **1** and **2**, [G1] OGD, and OG are about or less than half the intensity obtained from C8E4 (Figure 3B). This comparison should be regarded with caution because the technique used here is non-linear, and release efficiencies from the helium

droplets might vary between detergents. However, the observed absorption intensity differences can be used to qualitatively explain why higher laser energy is required to liberate membrane proteins from [G1] OGD and saccharide detergent micelles.[9c] The spectra also illustrate that fusing detergent headgroups into hybrid detergents does not result in a linear combination of their individual gas-phase IR spectra.

Computed vs Experimental Spectra

To understand the relationship between detergent structure and IR spectra, we sampled and optimized structures of the protonated detergents and computed harmonic IR spectra using density functional theory (DFT) at the PBE0 + D3/6-311 + G(d,p)[20] level of theory. All computed structures and IR spectra are provided in the Supporting Information.

The conformers and corresponding IR spectra yielding the best agreement between experiment and theory are shown in Figure 4 for the parent detergents C8E4, [G1] OGD, and OG. Due to the abundance of ether and hydroxyl groups, all structures show characteristic hydrogen bonding networks, which stabilize cyclic conformations. The lowest-energy computed conformer of C8E4 forms a ring comprising all oxygen atoms, in which the proton of the primary hydroxyl group and the additional proton are coordinated between the hydroxyl oxygen and the ether oxygens O3 and O5. This motif is found in all computed structures.

Similarly, in [G1] OGD, the proton bridges the primary hydroxyl group of one glycerol arm to the secondary hydroxyl group of the other arm, and the resulting cyclic structure is further stabilized by two additional hydrogen bonds. In OG, the proton is coordinated by the anomeric oxygen of glucose and stabilized by a hydrogen bonding network between all hydroxyl groups that lie on the same side of the sugar ring. The poor match between experiment and theory for this detergent will be discussed further below.

To determine how the hydrogen bond networks change when chemical groups are combined into a new molecule, structure optimization and frequency analysis of the hybrid detergents **1** and **2** were performed in the next step (Figure 5). The intramolecular interactions in detergent **1** contain elements of the interactions seen in [G1] OGD and C8E4: Similar to [G1] OGD, the two detergent arms are connected by an intramolecular hydrogen bridge between the two terminal hydroxyl groups. The hydroxyl protons are further coordinated by two ether oxygens like in C8E4. These are either O3 and O6 or O3 and O5 in the computed structures. The resulting structure can

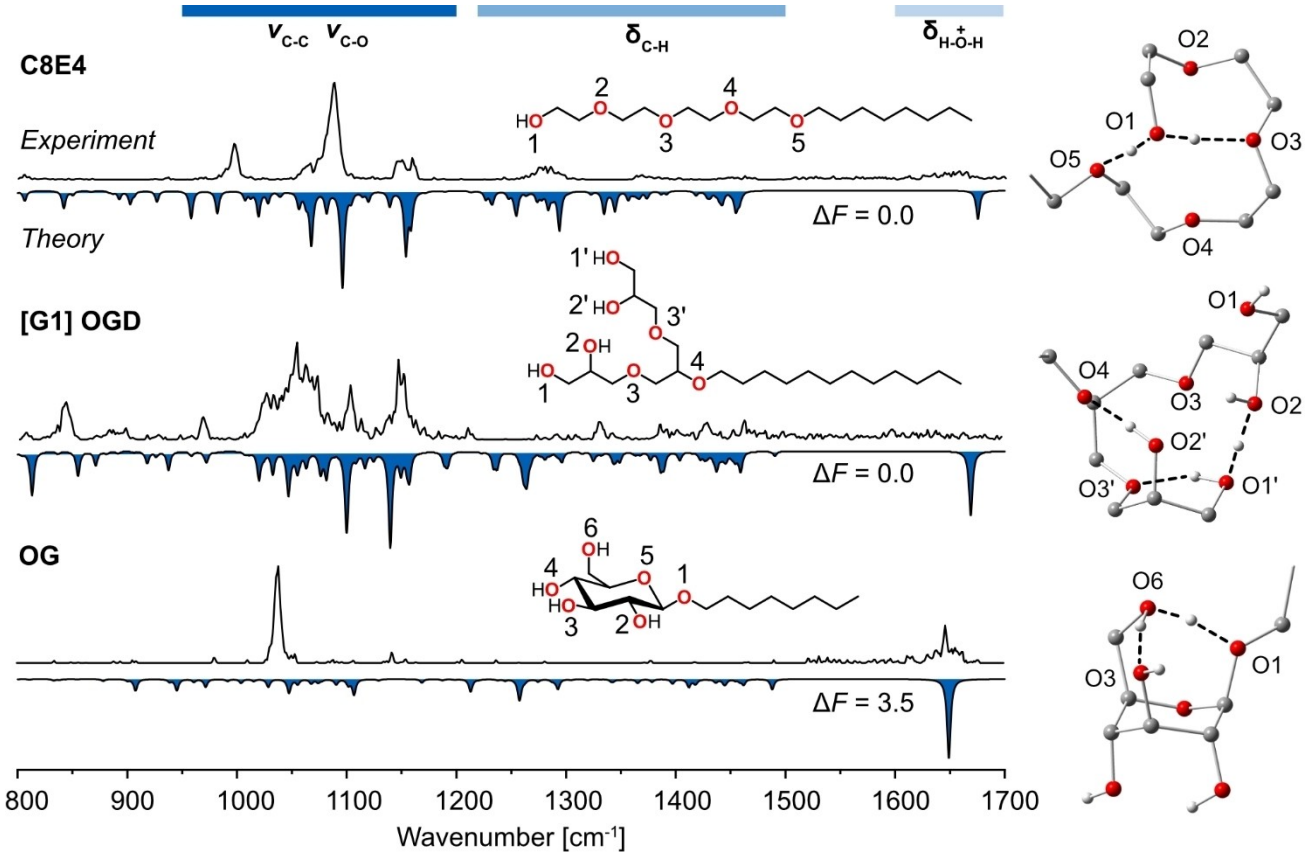

Figure 4. Optimized structures and computed infrared spectra (blue) compared with experimental IR spectra of parent detergents C8E4, [G1] OGD, and OG. Typical regions of stretching (ν) and bending (δ) vibrations observed in the spectra are indicated. The core interactions and relevant oxygen atoms are highlighted, with hydrocarbon chains truncated and aliphatic hydrogens removed for visibility. The computed free energies (ΔF) relative to the lowest-energy conformer are given in kJ mol^{-1}. Structure optimization and frequency analysis were performed at the PBE0 + D3/6-311 + G(d,p) level of theory and spectra were scaled by a factor of 0.965.

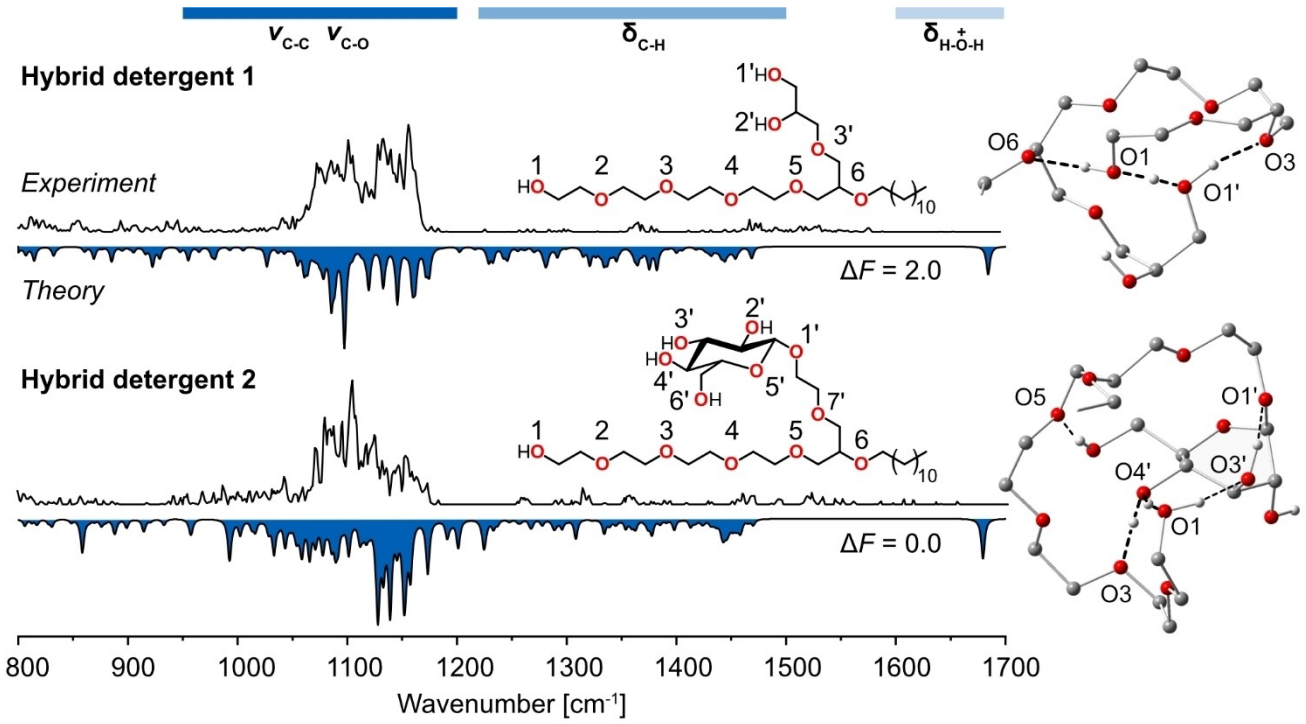

Figure 5. Computed infrared spectra and structures of hybrid detergents **1** and **2**. Typical regions of stretching (*ν*) and bending (*δ*) vibrations observed in the spectra are indicated. The core interactions and relevant oxygen atoms are highlighted with hydrocarbon chains truncated and aliphatic hydrogens removed for visibility. The glucose ring of hybrid detergent **2** is shaded for orientation in the computed structure. The computed free energies (Δ*F*) relative to the lowest-energy conformer are indicated in kJ mol^{-1}. Structure optimization and frequency analysis were performed at the PBE0 + D3/6-311 + G(d,p) level of theory and spectra were scaled by a factor of 0.965.

be described as tricyclic and is distinct from either of the conformations adopted by [G1] OGD and C8E4.

The conformation and IR spectrum of the glucose-containing hybrid detergent **2** significantly deviate from the OG subunit, because the inert hydrocarbon chain of OG is substituted by a C8E4 arm, which has the capacity to form hydrogen bonds. In all computed structures of hybrid detergent **2**, the proton forms a bridge between the sugar and the tip of the C8E4 chain: the C4 hydroxyl group of glucose forms hydrogen bonds to the primary alcohol at the tip of C8E4 and the ether oxygen O3. Furthermore, the C3 hydroxyl group of glucose forms hydrogen bonds with the anomeric oxygen (O1′) and the tip of C8E4, while the C6 hydroxyl group of the sugar forms a single hydrogen bond with O5 of the C8E4 chain. As a consequence of this dense hydrogen bonding network between hydroxyl groups of glucose and ether oxygens of C8E4, the polyethylene glycol chain is locked in a conformation in which the entire chain is wrapped around the sugar. Overall, the hybrid detergents show similar hydrogen bonding motifs as their constituent parent detergents but adopt largely different three-dimensional structures.

In Figures 4 and 5, we display only one of the lowest-energy conformers that yielded the best match with the experimental spectrum. However, since many computed structures differ by only a few kJ mol^{-1}, we expect that each spectrum represents an overlay of several low-energy conformers that coexist in the ion trap. Ion capture in superfluid helium droplets conserves the conformer distribution present at the ion trap temperature of 90 K because rapid cooling to 0.4 K prevents interconversion between conformers. For most detergents, except for OG, the overall appearance of the computed IR spectra is comparably insensitive to conformational changes such as different folding of the alkyl chain, as long as the core hydrogen bonds remain the same (Figures S2–6). Accordingly, a single conformer fits the experimental spectra reasonably well (Figure S7).

The absorption band that shifts most visibly between conformers corresponds to the H-O^{+}-H bending vibration between 1600–1700 cm^{-1}. This vibration involves a shared proton, which is known to be strongly anharmonic and thus not well predicted by the harmonic frequency calculations performed here.[18] Frequency shifts of this vibration between different conformers could explain why this particular absorption is broadened out and reduced in intensity in the experimental spectra: If multiple conformers with overall similar spectra but shifted H-O^{+}-H vibrations contribute to the experimental spectrum, they absorb over a broad range between 1600–1700 cm^{-1}. However, as only few ions absorb at each particular wavelength, the peak gets diluted in the combined IR spectrum.

In contrast to the other detergents, for OG we find that slight conformational changes cause significant differences in the appearance of the IR spectrum (Figures S4 and S8). Accordingly, the match between experiment and the computed spectrum of a single conformer is unsatisfactory (Figure 4). The conformation of the alkyl chain influences the absorption

properties of OG, which is curious as it is not involved in hydrogen bonding.

Overall, the results demonstrate that the appearance of a detergent's IR spectrum is highly dependent on its three-dimensional conformation, which is mainly determined by intramolecular interactions between heteroatoms. As a consequence, we expect the absorption properties of the same detergents in a micelle to be different from those of the isolated ions studied herein. Transferring our data on isolated molecules to detergent micelles is thus not directly possible. In addition to intramolecular hydrogen bonds, detergent molecules in micelles are expected to form intermolecular interactions with other detergent molecules and the protein. We suspect that these interactions are of similar nature as those observed for isolated detergents, *i. e.*, intermolecular hydrogen bonding between oxygen atoms of neighbouring detergent molecules and between detergents and protein residues. Because of the heterogeneity of protein-detergent complexes, the interactions will be promiscuous and lead to broadening of absorption bands, which potentially increases overlap with the IR laser.[9c]

Implications on Future Detergent Design

To answer the question that motivated this study – How do gas-phase IR spectra of detergents change when their headgroups are covalently fused into hybrid detergents? – we can say that detergents must contain certain functional groups to absorb in a specific region of the IR spectrum. However, the exact absorption patterns of hybrid detergents are not rationally predictable based on the IR spectra of their parent detergents. Even though the intramolecular interactions are similar in the constituent and fused hybrid detergents, the detergent's three-dimensional conformation changes significantly when hydrogen bond-forming groups are arranged in new combinations. Gas-phase IR spectroscopy is known to be extremely sensitive towards changes in the three-dimensional structure of molecules and can be used to identify optimal IRMPD wavelengths for each detergent.[21]

Regardless of the mass spectrometry application, detergents are optimized empirically, which involves the resource-consuming synthesis of detergent libraries and empirical tests.[3b,5a] We suggest that the need for synthesis of detergents with tailored gas-phase IR absorption properties can be guided by computational chemistry. Candidate structures could be generated and filtered for desired absorption properties *in silico* before their actual synthesis. Because different absorption properties are expected for isolated detergent molecules versus micellar detergent assemblies, we suggest as a next step that detergent assemblies should be taken into account in simulations, which increases computational cost but can yield results that are closer to reality.

Conclusion

Here we studied the absorption properties of five detergents that are commonly used for nMS of membrane proteins and investigated how absorption properties change when detergent headgroups are fused into hybrid detergents. Even though detergents assemble into micelles in nMS, we can derive several important conclusions from studying isolated detergent ions by gas-phase IR spectroscopy: First, for most detergents, the appearance of the IR spectrum is mainly determined by hydrogen bonds between heteroatoms, while the aliphatic tail has only a minor influence. Second, the hydrogen bonding network determines the three-dimensional conformation of the molecule, which can change significantly when hydrogen bond-forming functional groups are added or removed. Third, we conclude that rational design of detergents with desired absorption properties is challenging because IR absorption depends not only on the chemical groups present, but also on the interactions in the context of the detergent's environment, which are difficult to predict. The rational synthetic approach of combining chemical groups of detergents therefore does not automatically lead to a sum of their IR absorption properties. We propose that computational chemistry could help to identify candidate structures with desired absorption properties in detergent aggregates that mimic the micellar arrangement of detergents around membrane proteins.

Experimental Section

Detergent Synthesis

The detergents C8E4 and OG were purchased from Anatrace. [G1] OGD as well as the hybrid detergents **1** and **2** were synthesized following previously established procedures.[8,10]

Gas-Phase Infrared Ion Spectroscopy

The detergents were dissolved in a 1:1 (v:v) water/methanol solution and diluted to a final concentration of 200 μM for measurements. The instrument used for gas-phase IR ion spectroscopy has been described in detail in previous publications.[15] Detergent solutions are ionized by nano electrospray ionization using needles pulled from borosilicate capillaries by a P-1000 micropipette puller (Sutter Instrument, USA) and coated with Pd/Pt by a sputter coater 108auto (Cressington, Germany). The ionized detergents are guided through a quadrupole into a time-of-flight mass spectrometer to record mass spectra. For measurement of IR spectra, protonated ions are selected in the quadrupole and transferred to a hexapole ion trap filled with pre-cooled helium buffer gas (90 K). After thermalization of the ions, helium is pumped out of the trap. Superfluid helium droplets are generated by the expansion of pressurized helium (60 bar) through the cold nozzle of an Even-Lavie valve (21 K) operating at a frequency of 10 Hz. The droplets traverse the ion trap coaxially at a speed of 400–500 $m\,s^{-1}$ and pick up trapped ions. Due to their high kinetic energy of a few hundred eV, the doped droplets easily overcome the trapping potential of 3–5 V and leave the trap towards the interaction region. Here, the beam of doped droplets overlaps in space and time with the pulsed IR beam (10 Hz) of the Fritz Haber Institute free-electron laser.[17] If the wavelength of the laser corresponds to

a vibrational transition of the ion, multiple photons are sequentially absorbed, the vibrational energy is dissipated into the helium bath, and helium evaporates from the droplet until the ion is released or the droplet is completely evaporated. The droplet size distribution is a log-normal distribution with a mean size of 7×10^4 atoms per droplet under the employed experimental conditions.[22] Assuming that the energy required to remove one helium atom from the droplet is 5 cm^{-1},[23] about 230 photons are required for complete evaporation of an average-sized droplet at 1500 cm^{-1} photon energy, whereas the smallest 10% of droplets require only 110 photons.[24] After ion release or complete droplet evaporation, helium-free ions are detected by a time-of-flight mass spectrometer. IR spectra are generated by measuring the ion yield as a function of the laser wavelength (here 800–1700 cm^{-1}, 2 cm^{-1} steps). Each spectrum is averaged from two individual scans.

Computational Details

IR spectra of protonated detergents were generated in four steps involving the generation of protomers, conformational sampling of the lowest-energy protomer, structure optimization of generated conformers, and harmonic frequency analysis of the optimized structures. Protomers were generated with CREST[25] (version 2.9) and the semiempirical method GFN2-xTB[26] (xTB version 6.3.0) using the '-protonate' tool. All generated protomers were subjected to DFT optimization at the PBE0 + D3/6–31G(d)[20] level of theory in Gaussian 16 (rev. A.03).[27] In all cases the lowest-energy protomer was more stable in electronic energy than the second lowest by more than 30 kJ mol^{-1}. The lowest-energy protomer was subjected to a conformational analysis in CREST with the GFN2-xTB method, and the 60 most stable obtained conformers were optimized by DFT at the PBE0 + D3/6–31 G(d) level of theory in Gaussian 16. From this subset of DFT-optimized structures, the most stable 13–16 (24 for OG) conformers were selected for reoptimization at the PBE0 + D3/6-311 + G(d,p)[20] level of theory in Gaussian 16 using tight optimization settings.[27] Harmonic frequency analyses were performed for all selected conformers at the same level of theory. The resulting harmonic frequency spectra were scaled by an empirical factor of 0.965. Harmonic free energies (ΔF) were determined at a temperature of 90 K, according to the temperature in the ion trap.

Supporting Information Summary

Mass spectra of detergents, computed structures, and harmonic IR spectra are provided in the Supporting Information.

Acknowledgements

The Ministry of Culture and Science of the German State of North Rhine-Westphalia (NRW return program), Fonds der Chemischen Industrie, and Fonds National de la Recherche (FNR), Luxembourg (project GlycoCat; 13549747) are gratefully acknowledged for financial support.

Conflict of Interest

The authors declare no conflict of interest.

Keywords: Detergents · Membrane proteins · Mass spectrometry · Infrared multiple photon dissociation · Infrared spectroscopy

[1] a) R. R. O. Loo, N. Dales, P. C. Andrews, *Protein Sci.* **2008**, *3*, 1975–1983; b) N. P. Barrera, N. Di Bartolo, P. J. Booth, C. V. Robinson, *Science* **2008**, *321*, 243–246.
[2] A. Laganowsky, E. Reading, J. T. Hopper, C. V. Robinson, *Nat. Protoc.* **2013**, *8*, 639–651.
[3] a) J. E. Keener, G. Zhang, M. T. Marty, *Anal. Chem.* **2021**, *93*, 583–597; b) J. S. Behnke, L. H. Urner, *Anal. Bioanal. Chem.* **2023**, *415*, 3897–3909.
[4] a) E. Reading, I. Liko, T. M. Allison, J. L. Benesch, A. Laganowsky, C. V. Robinson, *Angew. Chem. Int. Ed.* **2015**, *54*, 4577–4581; b) L. H. Urner, I. Liko, K. Pagel, R. Haag, C. V. Robinson, *Biochim. Biophys. Acta Biomembr.* **2022**, *1864*, 183958.
[5] a) L. H. Urner, *Curr. Opin. Chem. Biol.* **2022**, *69*, 102157; b) L. H. Urner, F. Fiorentino, D. Shutin, J. B. Sauer, M. T. Agasid, T. J. El-Baba, J. R. Bolla, P. J. Stansfeld, C. V. Robinson, *J. Am. Chem. Soc.* **2024**, *146*, 11025–11030.
[6] a) R. J. Rose, E. Damoc, E. Denisov, A. Makarov, A. J. Heck, *Nat. Methods* **2012**, *9*, 1084–1086; b) J. Gault, J. A. Donlan, I. Liko, J. T. Hopper, K. Gupta, N. G. Housden, W. B. Struwe, M. T. Marty, T. Mize, C. Bechara, Y. Zhu, B. Wu, C. Kleanthous, M. Belov, E. Damoc, A. Makarov, C. V. Robinson, *Nat. Methods* **2016**, *13*, 333–336.
[7] A. J. Borysik, D. J. Hewitt, C. V. Robinson, *J. Am. Chem. Soc.* **2013**, *135*, 6078–6083.
[8] L. H. Urner, F. Junge, F. Fiorentino, T. J. El-Baba, D. Shutin, G. Nolte, R. Haag, C. V. Robinson, *Chem. Eur. J.* **2023**, *29*, e202300159.
[9] a) V. A. Mikhailov, I. Liko, T. H. Mize, M. F. Bush, J. L. Benesch, C. V. Robinson, *Anal. Chem.* **2016**, *88*, 7060–7067; b) B. R. Juliano, J. W. Keating, B. T. Ruotolo, *Anal. Chem.* **2023**, *95*, 13361–13367; c) C. A. Lutomski, T. J. El-Baba, J. D. Hinkle, I. Liko, J. L. Bennett, N. V. Kalmankar, A. Dolan, C. Kirschbaum, K. Greis, L. H. Urner, P. Kapoor, H. Y. Yen, K. Pagel, C. Mullen, J. E. P. Syka, C. V. Robinson, *Angew. Chem. Int. Ed.* **2023**, *62*, e202305694; d) I. D. Campuzano, H. Li, D. Bagal, J. L. Lippens, J. Svitel, R. J. Kurzeja, H. Xu, P. D. Schnier, J. A. Loo, *Anal. Chem.* **2016**, *88*, 12427–12436.
[10] L. H. Urner, A. Ariamajd, A. Weikum, *Chem. Sci.* **2022**, *13*, 10299–10307.
[11] F. Zhao, Z. Zhu, L. Xie, F. Luo, H. Wang, Y. Qiu, W. Luo, F. Zhou, D. Xue, Z. Zhang, T. Hua, D. Wu, Z. J. Liu, Z. Le, H. Tao, *Chemistry (Easton)* **2022**, *28*, e202201388.
[12] M. Yang, W. Luo, W. Zhang, H. Wang, D. Xue, Y. Wu, S. Zhao, F. Zhao, X. Zheng, H. Tao, *Chem. Asian J.* **2022**, *17*, e202200372.
[13] L. H. Urner, Y. B. Maier, R. Haag, K. Pagel, *J. Am. Soc. Mass Spectrom.* **2019**, *30*, 174–180.
[14] L. H. Urner, M. Schulze, Y. B. Maier, W. Hoffmann, S. Warnke, I. Liko, K. Folmert, C. Manz, C. V. Robinson, R. Haag, K. Pagel, *Chem. Sci.* **2020**, *11*, 3538–3546.
[15] a) A. I. González Flórez, E. Mucha, D. S. Ahn, S. Gewinner, W. Schöllkopf, K. Pagel, G. von Helden, *Angew. Chem. Int. Ed.* **2016**, *55*, 3295–3299; b) E. Mucha, A. I. González Flórez, M. Marianski, D. A. Thomas, W. Hoffmann, W. B. Struwe, H. S. Hahm, S. Gewinner, W. Schöllkopf, P. H. Seeberger, G. von Helden, K. Pagel, *Angew. Chem. Int. Ed.* **2017**, *56*, 11248–11251.
[16] D. Verma, R. M. P. Tanyag, S. M. O. O'Connell, A. F. Vilesov, *Adv. Phys.: X* **2019**, *4*, 1553569.
[17] W. Schöllkopf, S. Gewinner, H. Junkes, A. Paarmann, G. von Helden, H. Bluem, A. M. M. Todd, *Proc. SPIE* **2015**, *9512*, 95121L.
[18] D. A. Thomas, M. Marianski, E. Mucha, G. Meijer, M. A. Johnson, G. von Helden, *Angew. Chem. Int. Ed.* **2018**, *57*, 10615–10619.
[19] E. Mucha, D. Thomas, M. Lettow, G. Meijer, K. Pagel, G. von Helden, *in Molecules in Superfluid Helium Nanodroplets* (Eds: A. Slenczka, J. P. Toennies), Springer, Cham **2022**, *145*, 241–280.
[20] a) C. Adamo, V. Barone, *J. Chem. Phys.* **1999**, *110*, 6158–6170; b) S. Grimme, J. Antony, S. Ehrlich, H. Krieg, *J. Chem. Phys.* **2010**, *132*, 154104.
[21] C. Kirschbaum, K. Greis, E. Mucha, L. Kain, S. Deng, A. Zappe, S. Gewinner, W. Schöllkopf, G. von Helden, G. Meijer, P. B. Savage, M. Marianski, L. Teyton, K. Pagel, *Nat. Commun.* **2021**, *12*, 1201.
[22] A. I. González Flórez, *Biomolecular Ions in Helium Nanodroplets*, Freie Universität Berlin, Berlin **2016**.
[23] J. P. Toennies, A. F. Vilesov, *Angew. Chem. Int. Ed.* **2004**, *43*, 2622–2648.
[24] A. Y. Torres-Boy, M. I. Taccone, C. Kirschbaum, K. Ober, T. Stein, G. Meijer, G. von Helden, *J. Phys. Chem. A* **2024**, *128*, 4456–4466.

[25] P. Pracht, F. Bohle, S. Grimme, *Phys. Chem. Chem. Phys.* **2020**, *22*, 7169–7192.
[26] C. Bannwarth, S. Ehlert, S. Grimme, *J. Chem. Theory Comput.* **2019**, *15*, 1652–1671.
[27] M. J. Frisch, G. W. Trucks, H. B. Schlegel, G. E. Scuseria, M. A. Robb, J. R. Cheeseman, G. Scalmani, V. Barone, G. A. Petersson, H. Nakatsuji, X. Li, M. Caricato, A. V. Marenich, J. Bloino, B. G. Janesko, R. Gomperts, B. Mennucci, H. P. Hratchian, J. V. Ortiz, A. F. Izmaylov, J. L. Sonnenberg, D. Williams-Young, F. Ding, F. Lipparini, F. Egidi, J. Goings, B. Peng, A. Petrone, T. Henderson, D. Ranasinghe, V. G. Zakrzewski, J. Gao, N. Rega, G. Zheng, W. Liang, M. Hada, M. Ehara, K. Toyota, R. Fukuda, J. Hasegawa, M. Ishida, T. Nakajima, Y. Honda, O. Kitao, H. Nakai, T. Vreven, K. Throssell, J. A. Montgomery Jr., J. E. Peralta, F. Ogliaro, M. J. Bearpark, J. J. Heyd, E. N. Brothers, K. N. Kudin, V. N. Staroverov, T. A. Keith, R. Kobayashi, J. Normand, K. Raghavachari, A. P. Rendell, J. C. Burant, S. S. Iyengar, J. Tomasi, M. Cossi, J. M. Millam, M. Klene, C. Adamo, R. Cammi, J. W. Ochterski, R. L. Martin, K. Morokuma, O. Farkas, J. B. Foresman, D. J. Fox, *Gaussian 16, Rev. A.03*, Gaussian, Inc., Wallingford CT, **2016**.

Manuscript received: May 14, 2024
Revised manuscript received: June 20, 2024
Version of record online: August 8, 2024